



City Research Online

City, University of London Institutional Repository

Citation: Tomas-Rodriguez, M. & Moreno-Ramirez, C. (2018). Dynamic Analysis of Double Wishbone Front Suspension Systems for Sport Motorcycles. *Nonlinear Dynamics*, 91(4), pp. 2437-2368. doi: 10.1007/s11071-017-4017-9

This is the accepted version of the paper.

This version of the publication may differ from the final published version.

Permanent repository link: <https://openaccess.city.ac.uk/id/eprint/18640/>

Link to published version: <https://doi.org/10.1007/s11071-017-4017-9>

Copyright: City Research Online aims to make research outputs of City, University of London available to a wider audience. Copyright and Moral Rights remain with the author(s) and/or copyright holders. URLs from City Research Online may be freely distributed and linked to.

Reuse: Copies of full items can be used for personal research or study, educational, or not-for-profit purposes without prior permission or charge. Provided that the authors, title and full bibliographic details are credited, a hyperlink and/or URL is given for the original metadata page and the content is not changed in any way.

Dynamic Analysis of Double Wishbone Front Suspension Systems for Sport Motorcycles

Ciro Moreno Ramírez
Department of Mechanical
Engineering and Aeronautics
City, University of London
United Kingdom
Moreno.Ciro.1@city.ac.uk

M. Tomás-Rodríguez
Department of Mechanical
Engineering and Aeronautics
City, University of London
United Kingdom
Maria.Tomas-Rodriguez.1@city.ac.uk

Simos A. Evangelou
Electrical and Electronic
Engineering Department
Imperial College
London
United Kingdom
S.Evangelou@imperial.ac.uk

In this paper, two alternative front suspension systems and their influence on motorcycle dynamics are investigated. Based on an existing motorcycle mathematical model, the front end is modified to accommodate both Girder and Hossack suspension systems. Both of them have in common a double wishbone design that varies the front end geometry on certain manoeuvrings and, consequently, the machine's behaviour. The kinematics of the two systems and their impact on the motorcycle performance is analysed and compared to the well known telescopic fork suspension system. Stability study for both systems is carried out by means of root-loci methods, in which the main oscillation modes, weave and wobble, are studied and compared to the baseline model.

Nomenclature

wb Motorcycle wheelbase.

ϵ Motorcycle head angle.

t Motorcycle trail.

t_n Motorcycle normal trail.

ofs Front wheel offset from the steering axis.

prl 'Parallelogram' geometrical configuration of the double wishbone front suspensions.

tft 'Telescopic fork's trajectory' geometrical configuration of the double wishbone front suspensions.

cnt 'Constant normal trail' geometrical configuration of the double wishbone front suspensions.

$v.s.t.$ Vertical suspension travel.

Z_{hb} Vertical displacement of the handlebar.

Z_{fw} Vertical displacement of the front wheel.

1 Introduction

The motorcycle's front end links the front wheel to the motorcycle's chassis and has two main functions: the front wheel suspension and the vehicle steering. Up to this date, several suspension systems have been developed in order to achieve the best possible front end behaviour, being the telescopic fork the most common one.

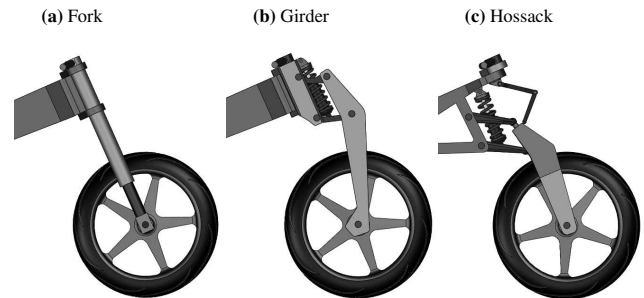


Fig. 1: 3D models of Fork (a), Girder (b) and Hossack (c) suspension systems.

A telescopic fork 3D model can be observed in Fig. 1a. It consists of a couple of outer tubes which contain the suspension components (coil springs and dampers) internally and two inner tubes which slide into the outer ones allowing the suspension travel. The outer tubes are attached to the frame through two triple trees which connect the front end to the main frame through the steering bearings and allow the front wheel to turn about the steering axis. This system keeps

the front wheel's displacement in a straight line parallel to the steering axis. However, there exist alternative suspension designs that allow different trajectories of the front wheel with the suspension travel. These systems can be divided into two main groups. The first of them presents the steering axle located between the chassis and the suspension elements (wishbones in most of the cases). In the second group, this axle is placed between the suspension elements and the front wheel. In both cases, the system can be designed in order to provide a desired front wheel trajectory, however whilst the first group keeps the steering angle fixed in the chassis reference frame, the second one modifies it with the travel of the suspension. Two double wishbone systems are considered in this research as representative of these two groups: the Girder suspension and the Hossack system respectively. 3D models of these suspension systems are shown in Figure 1.

The Girder suspension system (Fig. 1b) consists of a pair of long uprights where the front wheel is attached to. These uprights are linked to the triple trees by an upper and a lower wishbones which perform the suspension motion. Both triple trees rotate about the steering axle which is fixed to the motorcycle chassis. A spring-damper unit is usually attached between the lower wishbone and the upper triple tree providing the shock absorption function. On the other hand, the Hossack suspension system (Fig. 1c) consists of a double wishbone structure directly attached to the chassis. The two wishbones rotate both about axles perpendicular to the symmetry plane of the motorcycle, providing the suspension motion. An upright is linked to the front tips of the wishbones by two ball joints, which allow it to turn left and right as well as to move up and down. Therefore, the steering axis becomes defined by the imaginary line passing through the geometric centre of the ball joints. The control over the steering angle is applied by the rider to the handlebar which is connected to the upright through the steering linkage. This is a system of two levers, connected by an axis, which can be compressed or elongated in order to reach the length between the handlebar and the upright. The front wheel is attached to this upright and the suspension reaction is provided by a spring-damper unit attached between the lower wishbone and the motorcycle chassis. In terms of kinematics, these two types of designs cover most of the existing double wishbone suspension system.

The main goal of this research is to study the effects of alternative front suspension systems on motorcycle dynamics. That is, how the different modifications introduced by the new suspension systems, such as different mechanical designs or changes in the front end geometry with new wheel trajectories, affect the suspension response and the motorcycle stability. The framework of this research is the mathematical modelling and numerical simulation. We took advantage of a high fidelity motorcycle model developed by [1] which has been modified with the addition of the alternative suspension system under study. The motorcycle model properties and the simulation tools used during this research are explained in section 2.

In order to obtain realistic descriptions of the alternative front suspension systems in terms of dynamical properties,

we have designed and modelled these systems taking advantage of CAE tools. As a first step, the kinematics of the two systems are studied in comparison with the telescopic fork. Then, different kinematic configurations are synthesized taking into consideration different aspects of the front end geometry. This part of the research is explained in section 3. The second step consists in 3D design and compliance analysis of the suspension systems. This process allows to obtain exact values of the systems' parts dynamical properties (such as masses and moments of inertia) of realistic suspension designs. Once the dynamical properties of all the suspension systems' parts are obtained, the motorcycle model was modified to include the new suspension systems. This dynamical modelling process is explained in section 4. Several simulations were carried out with the new motorcycle models in order to test the suspension response under different conditions (section 5). Full stability analyses were performed to identify and reduce the eventual stability risks that the new suspension systems may introduce in the motorcycle dynamics (section 6). Finally, conclusions of this research are presented in section 7.

2 Motorcycle model and simulation tools

The different mathematical models developed for this research are based on the model presented in [1]. This mathematical model was built during several years of research underpinned by wide literature and experimental data. This model has been extensively used in the past in several contributions such as [2], [3], [4], [5], [6] and [7]. Furthermore, it has been widely tested and adopted by the industry. For instance, BikeSim software [8] is a motorcycle dynamics simulator which is based on this model and it is used by a large number of manufacturers to obtain high fidelity prediction on the dynamics of their machines.

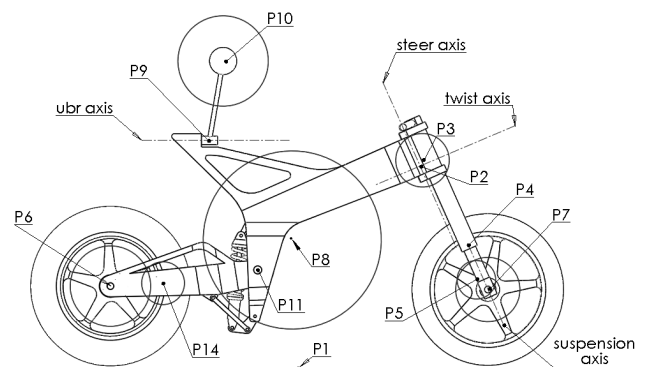


Fig. 2: GSX-R1000 geometrical description. Blue circles with diameter proportional to body mass are plotted around the centre of mass of each body.

The model was developed using real dynamical parameters of an existing motorcycle. The Suzuki GSX-R1000 K1 superbike, with 170 kg of mass, powered by an in-line four cylinder and four stroke engine with 988 cc able to deliver

160 hp, this machine is a good representative of contemporary commercial high performance motorcycles.

Point	Description
P1	Aerodynamic reference point.
P2	Twist body's joint with rear frame.
P3	Steer body's centre of mass.
P4	Front suspension body's joint with steer body.
P5	Front suspension body's centre of mass.
P6	Front wheel's centre of mass and attachment point.
P7	Rear wheel's centre of mass and attachment point.
P8	Main frame's centre of mass.
P9	Rider's Upper Body attachment point on rear frame
P10	Centre of mass of the rider's upper body.
P11	Swinging arm's attachment point on main frame.
P14	Swinging arm's centre of mass.

Table 1: GSX-R1000 geometrical model main points.

The motorcycle model consists of seven bodies: rear wheel, swinging arm, main frame (comprising rider's lower body, engine and chassis), rider's upper-body, steering frame, telescopic fork suspension and front wheel. It involves 13 degrees of freedom: three rotational and three translational for the main frame, two rotational for the wheels spin, one rotational for the swinging arm, one rotational for the rider's upper body, one rotational for the frame flexibility, one rotational for the steering body and one translational for the front suspension fork. Figure 2 represents the main geometric points and axes in the motorcycle's geometry. The centre of mass of each of the seven constituent bodies is represented as a blue circle with a diameter proportional to its mass. Table 1 contains the indexes of these points. For modelling purposes, a parent-child structure is used, as shown in Fig. 3.

The tires are treated as wide, flexible in compression and the migration of both contact points as the machine rolls, pitches and steers is tracked dynamically. The tyre's forces and moments are generated from the tyre's camber angle relative to the road, the normal load and the combined slip using Magic Formulae models [9] and [10]. This model is applicable to motorcycle tires operating at roll angles of up to 60° .

The aerodynamic drag/lift forces and pitching moment are modelled as forces/moments applied to the aerodynamic centre and they are proportional to the square of the motorcycle's forward speed. In order to maintain steady-state operating conditions, the model contains a number of control systems, which mimic the rider's control action. These systems control the throttle, the braking and braking distribution between the front and rear wheels, and the vehicle's steering.

The forward speed is maintained by a driving torque applied to the rear wheel and reacting on the main frame. This torque is derived from a proportional-integral (*PI*) controller on the speed error with fixed gains.

For some manoeuvres, the motorcycle is not self-stable;

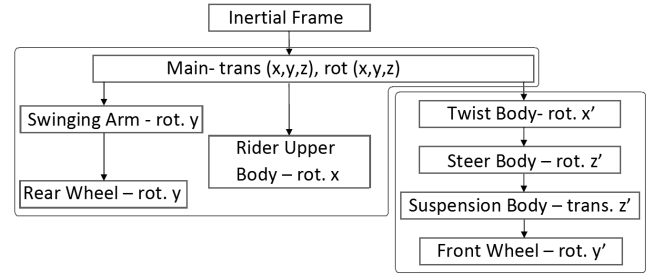


Fig. 3: Parental structure of the GSX-R1000 model.

in order to stabilise the machine in such situations a roll angle feedback controller is implemented. This allows to obtain different steady turning equilibrium states through simple simulations, which will not be stable without the roll angle controller. The controller developed was a proportional-integral-derivative (*PID*) feedback of motorcycle lean angle error to steering torque. The lean angle target is set by an initial value and a constant change rate. Thus, the target lean angle is a ramp function of time which can be easily modified. The *PID* gains are defined as speed adaptive in order to achieve an effective stabilisation of the motorcycle for the difficult cases involving very low or very high speeds. Finally, the steering control torque is applied to the steer body reacting on the rider's upper body.

Some modification to the baseline model have been applied for this research regarding the acceleration/braking systems and road inputs. In order to study the response of the new suspensions and their anti-dive properties, a braking system capable of delivering a constant deceleration was implemented. In the new system, the braking torque is derived from the *PI* controller on the speed error. On the other hand, the road input into the motorcycle tyres is also redefined. With the new approach, the longitudinal contact point migration produced by a step bump is included in the dynamic description and its effects on the suspension response are considered. More details on how this modifications were implemented can be found in [11].

The motorcycle model is implemented taking advantage of the VehicleSim multi-body software from Mechanical Simulation Corporation [8]. This suite consists of two separated tools: VS Lisp and VS Browser. VS Lisp is the tool used to generate the equations of motions from a multi-body description of any dynamical system. Making use of its own computer language (based on LISP) it is designed to automatically generate computationally efficient simulation programs for those multi-body systems. It can be configured to return either the corresponding non-linear equations of motion or the linearised equations of motion. Both non-linear and linearised equations of motion are symbolically described as functions of all the parameters defining the model dynamics, such as suspensions or aerodynamics coefficients.

With the non-linear equations of motion, a solver can be built with the same architecture and behaviour as those existing in commercial packages such as BiekSim and fully com-

patible with the VS Browser. VS Browser is the front end of all the VehicleSim products. It provides a graphical context with a standard graphical user interface from which the non-linear simulations can be run and the different databases can be managed. This includes the solvers created with VS Lisp, the external inputs and events and the data post processing and visualization.

On the other hand, the linearised equations of motion are returned in a Matlab file with the state space description of the systems. The state space matrices obtained (A, B, C and D) depend on both the system parameters and the state variables values. This feature become useful in the stability analysis of complex non linear systems, which can be linearised about operating points corresponding to quasi-equilibrium states. The frequency and damping associated to the system's normal modes are found through the matrix A eigenvalues. The previous version of this software was called Autosim and was already used in the past in motorcycles multi-body modelling (see [12] and [13]).

In this research, following the approach of previous works such as [5] or [14], the system's eigenvalues are plot in the complex plane for different values of the motorcycle speed and roll angle. In this way a general understanding on the stability properties of the different motorcycle models can be obtained. To do so, the non-linear equations of motions returned by VS Lisp are integrated under a quasi-equilibrium variation of the forward speed to obtain time histories of the state variables, for either straight running conditions or steady turns. Then, the state space matrix A can be fed with those values of the state variables for each time step, obtaining an accurate linear description of the motorcycle system for different forward speeds and roll angles. Speed and roll angle feedback controllers are used to reach the equilibrium states during the non-linear simulation. However, in the model's state space description these feedback controls are disabled in order to study the open-loop system stability. In section 6 this technique is used to study the variation in the root locus of the motorcycle model introduced by double wishbone suspension systems. That is, the effects on the stability of the motorcycle and its normal modes.

3 Front End Kinematics

Motorcycle handling properties are greatly influenced by some geometric parameters which are defined by the front end design. Figure 4 presents the four most relevant geometric parameters for motorcycle handling. These are the trail (t), the normal trail (t_n), the head angle (ϵ) and the wheelbase (wb). The wheelbase is the distance between the front and rear wheels contact points. The head angle is the angle between the steering axis and the vertical. The trail is the distance between the front wheel contact point and the point where the steering axis intersects with the ground. The normal trail is the projection of the trail distance into a plane perpendicular to the steering axis. This is the lever arm of the front tyre forces appearing on its contact point, which result in a torque about the steering axis. The normal trail (t_n) and the head angle (ϵ) are related to each other by

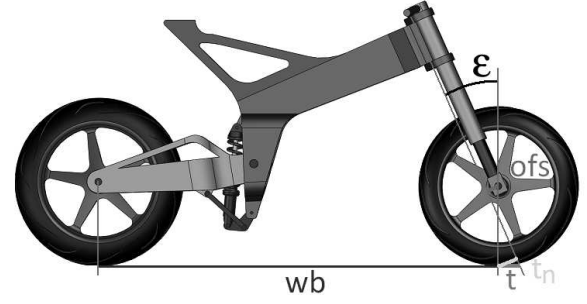


Fig. 4: Main motorcycle's handling geometric parameters. The wheelbase (wb) is plotted in brown, the trail (t) is in magenta, the normal trail (t_n) is in green, the head angle (ϵ) is in black and the fork offset (ofs) is shown in blue.

the following expression:

$$t_n = r_{fw} \cdot \sin(\epsilon) - ofs, \quad (1)$$

where r_{fw} is the tyre's radius and ofs is the front wheel's spindle offset from the steering axis. The wheelbase also depends on the rear frame construction including the swinging arm. In the case of a conventional telescopic fork, the steering axle is rigidly inserted into the chassis whilst the offset is a constant value. Therefore, when the fork is compressed the wheelbase and the head angle decrease and, thus, the trail and the normal trail. The vertical suspension travel ($v.s.t.$) is defined as the vertical travel of the front wheel centre when the suspension system is compressed ($v.s.t. > 0$) or extended ($v.s.t. < 0$) considering the chassis fixed in the inertial frame.

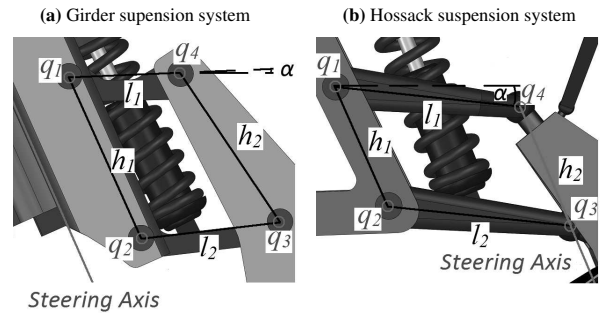


Fig. 5: Design parameters on the four-bar linkage suspension systems. a) Girder suspension system. b) Hossack suspension system.

This definition is valid for all the different suspension systems and provides a general magnitude that can be used to compare various behaviours.

Both Girder and Hossack systems consist in a four-bar linkage. The difference between them is the edge of the quadrilateral to be considered as steering axis. Figure 5 shows the design parameters of the four-bar linkage for these

two systems: the lengths of the upper (l_1) and lower (l_2) wishbones, the distances between the attachment points of the wishbones (h_1 on the chassis side and h_2 on the uprights side) and the angle between the upper wishbone and the horizontal at the nominal position (α). With these five parameters full assembly kinematics are defined. The variation of one of them will affect the overall behaviour of the handling geometric parameters with the suspension travel. Different configurations of these five parameters can be calculated to obtain different behaviours of the front suspension systems.

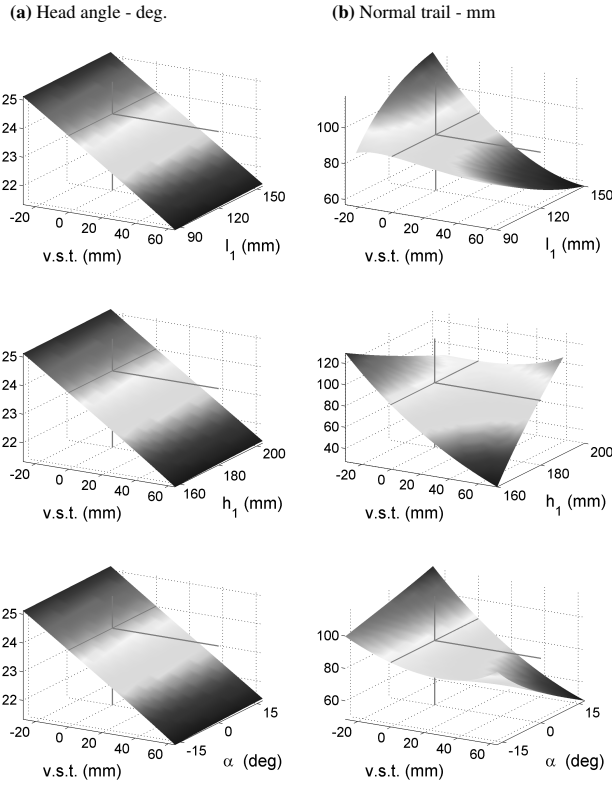


Fig. 6: Effects of varying the design parameters on the head angle and the normal trail for the **Girder** suspension system.

The impact on the kinematic behaviour of varying each design parameter value on the handling geometric parameters can be mapped. As an example, Fig. 6 shows the effects of modifying l_1 , h_1 and α parameters on the variation, with the vertical suspension travel, of the head angle and the normal trail for the Girder suspension system. Only the normal trail will be taken into consideration as it is the actual lever arm of the front wheel force about the steering axis, whilst the trail can be obtained as a simple function of the former as:

$$t = \frac{t_n}{\cos(\epsilon)} \quad (2)$$

As it can be expected, as the steering axle is fixed to the chassis, the head angle variation behave similarly with different values of any of the design parameters. However, the normal trail variation is affected by these parameters values. The Girder suspension system can be designed to perform a prescribed behaviour of the wheelbase and the normal trail whilst the head angle behaviour cannot be modified.

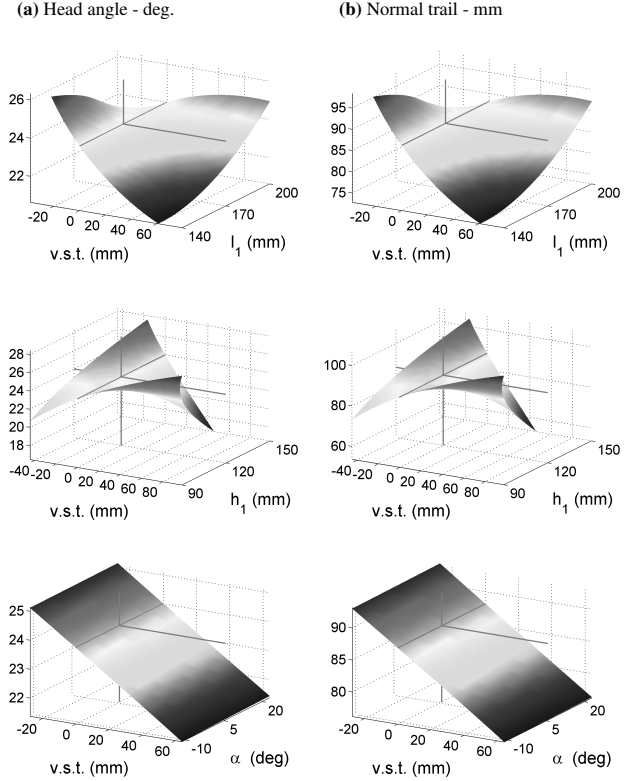


Fig. 7: Effects of varying the design parameters on the head angle and the normal trail for the **Hossack** suspension system.

Similar results are shown in Fig. 7 for the Hossack system. In this case, a close relation between the head angle and the normal trail behaviours can be observed due to the variable steering axis and the constant offset. The head angle and the normal trail keep their nominal response for different values of α but are significantly modified when other design parameters are varied. It is possible to obtain a desired head angle variation given certain vertical suspension travel with the Hossack suspension system, whilst the trail and the normal trail are closely related to it.

As it has been said, double wishbone suspension systems can be design with different kinematic behaviours. In order to study the effect of the front suspension systems' kinematic behaviour on the motorcycle dynamics, three main kinematic configurations are considered for both the Girder and Hossack suspension systems. The design parameters required for each of these configurations are obtained following a synthesis of mechanisms methodology, described in [11]. Several optimization processes were developed for

the different suspension systems taking advantage of Matlab's optimization toolbox, which was proven to be an adequate framework for this kind of problems. The following kinematic configurations were obtained:

- Parallelogram (*prl*): The suspension systems are designed with l_1 , l_2 , h_1 and h_2 as two pairs of parallel sides and with $\alpha = 0$, being this the simplest configuration. No optimization process is needed and the parallelogram's sides lengths are chosen within the space restrictions imposed by the motorcycle's design.
- Telescopic fork's trajectory (*tft*): The suspension systems are designed to obtain a front wheel trajectory similar to that followed by the front wheel with a telescopic fork system.
- Constant normal trail (*cnt*): The suspension systems are designed to obtain a constant normal trail along the full suspension travel.

The values of the design parameters obtained are given in Table 2 and Table 3, where l_1 , l_2 , h_1 and h_2 are expressed in mm and α is in degrees.

Girder configurations	l_1	l_2	h_1	h_2	α
Parallelogram	120	120	180	180	0.0
Fork trajectory	107	135	171	172	0.0
Constant t_n	106	131	192	185	0.0

Table 2: Design parameters values obtained for the three different Girder suspension systems configurations. l_1 , l_2 , h_1 and h_2 are expressed in mm and α is expressed in degrees.

Hossack configurations	l_1	l_2	h_1	h_2	α
Parallelogram	170	170	120	120	5.7
Fork trajectory	155	183	127	117	5.8
Constant t_n	173	190	102	123	6.0

Table 3: Design parameters values obtained for the three different Hossack suspension systems configurations. l_1 , l_2 , h_1 and h_2 are expressed in mm and α is expressed in degrees.

Figure 8a shows the handling geometric parameters behaviour of the Girder (green +) and Hossack (red x) suspension systems with parallelogram (*prl*) configuration compared with the telescopic fork (solid blue). It can be observed that with both double wishbone suspension systems the head angle (ϵ) variation mostly follows that of the telescopic fork. Regarding to the normal trail (t_n), its behaviour with the Hossack system is similar to that with the telescopic fork, whilst the Girder suspension presents a more pronounced decrease of this parameter with the vertical suspension travel

(*v.s.t.*). Finally the wheelbase (*wb*) behaves similarly with both Girder and Hossack suspension systems. This value is always reduced relative to the nominal position although in a less relevant manner, compared to the telescopic fork.

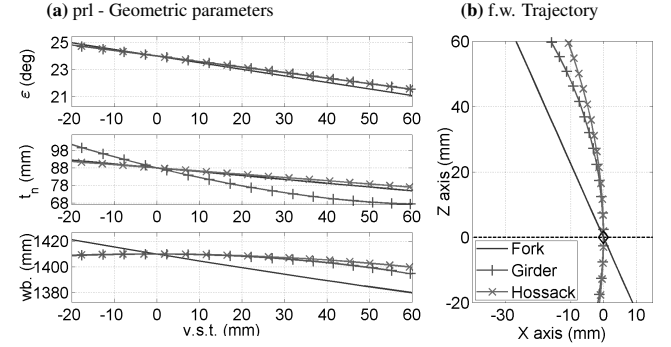


Fig. 8: Kinematic behaviour of the Girder (green +) and Hossack (red x) suspension systems with *prl* configuration compared with the telescopic fork (solid blue). The head angle (ϵ), the normal trail (t_n) and the wheelbase (*wb*) variation with the vertical suspension travel (*v.s.t.*) are presented in a). The front wheel contact point trajectories along the full suspension travel are plotted in b).

Figure 8b shows the trajectories of the front wheel contact points along the full suspension travel obtained with parallelogram configuration of the double wishbone suspension systems compared to that of the telescopic fork. Both Girder and Hossack systems produce curved trajectories. These trajectories are close to each other, have positive slopes between -20 mm and +10 mm of *v.s.t.* and differ from the nominal trajectory returned by the telescopic fork, which has constant negative slope.

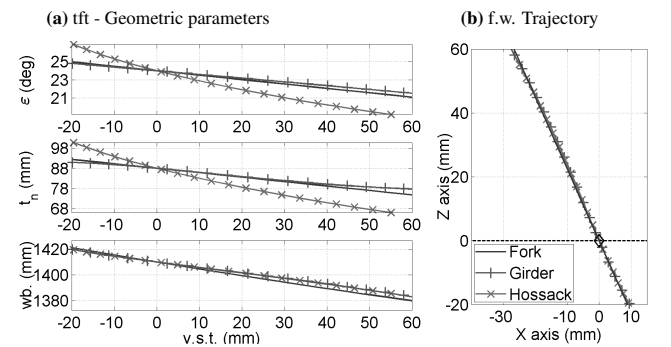


Fig. 9: Kinematic behaviour of the Girder (green +) and Hossack (red x) suspension systems with *tft* configuration compared with the telescopic fork (solid blue). The head angle (ϵ), the normal trail (t_n) and the wheelbase (*wb*) variation with the vertical suspension travel (*v.s.t.*) are presented in a). The front wheel contact point trajectories along the full suspension travel are plotted in b).

Similar plots are obtained for the Girder and Hossack suspension systems with telescopic fork's trajectory configuration (*tft*) in Fig. 9. The trajectories reached by both double

wishbone suspension systems are almost identical to that of the telescopic fork (Fig. 9b). In the case of the Girder suspension system, the handling geometric parameters behave similarly to those with the telescopic fork suspension (Fig. 9a). This is the expected behaviour as the steering axle and the wheel trajectories are equal in both systems. However, for the Hossack suspension system, the steering axle varies with the suspension travel, which leads to different behaviours of the handling geometric parameters. The variation in the head angle and the normal trail with the vertical suspension travel are significantly larger for the Hossack system than for the telescopic fork suspension. However, the wheelbase is modified in a similar way, as the front wheel follows the same trajectory in both cases.

Being the normal trail a crucial parameter in the motorcycle handling, it could be an interesting feature for a suspension system to maintain this value constant at any position of the suspension travel. Kinematic behaviours of the Girder and Hossack suspension systems with a constant normal trail configuration (*cnt*) are represented in Fig. 10a. Almost constant normal trails are achieved by both Girder and Hossack suspension systems, with small deviations from their nominal values. As expected, in the case of the Girder suspension, the head angle maintains its nominal behaviour with the vertical suspension travel whilst the wheelbase is reduced. However, the Hossack suspension system with *cnt* configuration returns an almost constant head angle and, oppositely to the Girder and telescopic fork systems, the wheelbase is increased in compression and decreased in extension.

Regarding to the front wheel's contact point in Fig. 10b, it can be observed that with the Girder system, the trajectory is mostly a straight line at an angle with the vertical which is greater than that of the telescopic fork's trajectory. In the case of the Hossack system, the front wheel follows a curved trajectory. The angle with the vertical becomes negative in this case, reducing its value under compression and increasing it under extension. These trajectory angles will directly affect the suspension systems' anti-dive capabilities. Contrary to the behaviour of the telescopic fork system, both double wishbone suspension systems show a wide range of possible kinematic configurations. Either Hossack or Girder systems could be a good choice depending on the motorcycle's kinematics requirements.

4 Dynamical modelling

In order to study the Girder and Hossack suspension systems' dynamic properties, two mathematical models have been built using VehicleSim. Each of these models geometry has been modified with the design parameters values obtained in the previous section for the three kinematic configurations: parallelogram (*prl*), telescopic fork's trajectory (*tft*) and constant normal trail (*cnt*). Therefore, three different configurations of each of the Girder and Hossack suspension systems are obtained.

The mathematical models here presented are developed as modifications of the Suzuki GSX-R1000 nominal model, derived in [1], which was built considering the actual physi-

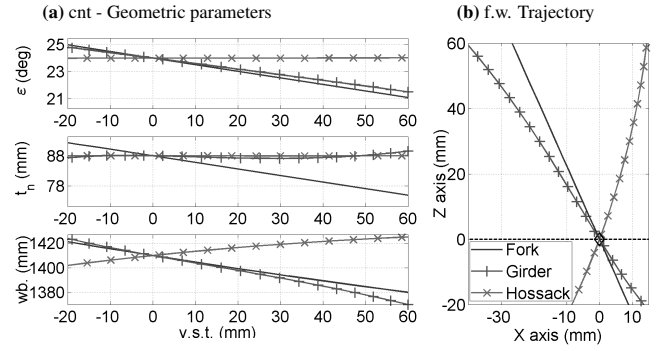


Fig. 10: Kinematic behaviour of the Girder (green +) and Hossack (red x) suspension systems with *cnt* configuration compared with the telescopic fork (solid blue). The head angle (ϵ), the normal trail (t_n) and the wheelbase (wb) variation with the vertical suspension travel (*v.s.t.*) are presented in a). The front wheel contact point trajectories along the full suspension travel are plotted in b).

cal properties of the original motorcycle's parts. The masses, the moments of inertia and the centres of masses were directly measured for each part. However, real GSX-R1000 motorcycles are not fitted with either Girder or Hossack suspensions. Therefore, the physical properties of these parts cannot be measured and included in the mathematical model. In order to obtain accurate values of these properties, a 3D computer-aided design (CAD) has been developed for each suspension system. The software used for this task was SolidWorks [15], which also allowed to perform the different compliance analyses (FEA) through its SolidWorks Simulation tool, needed to determine the designs consistency and reliability.

4.1 3D design and compliance analysis

It is important to note that this part of the research is not intended to obtain high performance commercial suspension systems, but to provide a good approximation of the mechanical parts involved on each suspension system under study. Therefore, the masses, the centre of masses, the inertia moments, etc. represent close values to those of a possible real suspension system implementation.

Both Girder and Hossack suspension systems are designed in order to keep the same front end assembly's mass as that of the original telescopic fork of the GSX-R1000 model. Each part's mass tends to be equal to the equivalent part in the telescopic fork case. However, due to the structural differences between the three suspension systems, this is not always possible. For instance, in the case of the Hossack suspension, the steering assembly consists only of a triple tree. This makes the Hossack systems much lighter than the telescopic fork's system. The Girder suspension is only a few grams lighter than the telescopic fork. Nevertheless, in both Girder and Hossack cases the mass difference is added to the chassis body as a mass placed at the same coordinates as those of the steering body's centre of mass.

A construction material is associated to the different parts of the suspension systems, so that the dynamic prop-

erties of each part can be calculated. The material chosen for both Girder and Hossack suspension systems was 7075 aluminium alloy, commonly used in automotive industry due to its strength and light weight. The suspension systems have been designed in order to support maximum loads during extreme running condition. Various finite element analyses were carried out for each suspension system in order to ensure their integrity and reliable performance under those heavy loads. Figure 11 show some examples of the FEA results for the Girder and Hossack suspension systems. For a more detailed explanation on the FEA analysis process the reader is refer to [11].

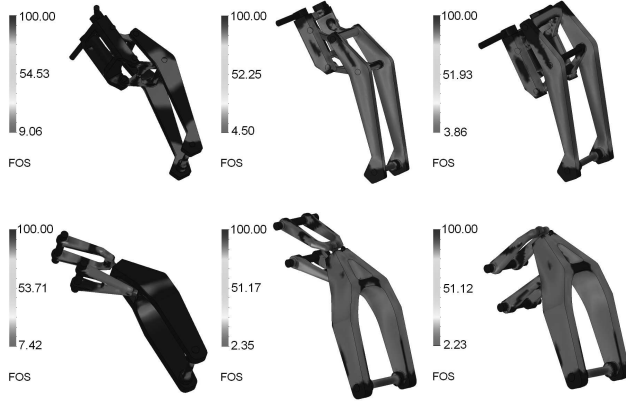


Fig. 11: Some examples of FEA results for the Girder and Hossack models.

In order to obtain a coherent comparison between the three different suspension systems, they have been divided in four subsystems each of them containing different parts. The parts belonging to each subsystem depend on which suspension system is considered.

STR: It is the body that allows the steering action. It comprises the triple trees and eventually other parts depending on the model under consideration. In the case of the telescopic fork it also includes the upper tubes. In the case of the Girder, the mass of the upper part of the spring damper unit is also included. In the case of the Hossack system, it includes the upper lever of the steering linkage.

SUS: It represents the body holding the front wheel. In the case of the telescopic fork it comprises the lower tubes of the fork. In the case of the Girder and Hossack suspension systems, this body corresponds to the uprights, the lower part of the spring-damper unit and, only for the Hossack system, the lower lever of the steering linkage.

UWB: This part is exclusively defined for the Girder and Hossack systems. It only consists of the upper wishbone.

LWB: This part is exclusively defined for the Girder and Hossack systems. It only consists of the lower wishbone.

The dynamic properties of each subsystem can be obtained from the 3D model in SolidWorks. Table 4 shows the masses of each part on the different suspension systems compared to the original telescopic fork parts masses. In the case of the Hossack system, the remaining mass needed to equal that of the original telescopic fork is 7.022 kg. However, as it has been said, an equivalent mass is added to the chassis body in the same coordinates than those of the steering body's centre of mass maintaining the overall motorcycle mass for both suspension systems.

mass (kg)	STR	SUS	UWB	LWB	Total
Fork	9.990	7.250	—	—	17.240
Girder	7.863	7.930	0.666	0.764	17.223
Hossack	1.1692	7.1489	0.976	0.924	10.218

Table 4: Masses for the different suspension systems models bodies

4.2 Mathematical modelling

The GSX-R1000 model presented in section 2 has been modified to include multi-body representations for both the Girder and the Hossack suspension systems. In both cases, and similarly to the original nominal model, a massless body is included (the twist body) that represents the frame's flexibility. The flexibility is defined as a rotational degree of freedom between the motorcycle chassis (rear frame) and the front suspension (front frame) about the twist axis. This is an axis perpendicular to the steering one which lies within the motorcycle's symmetry plane and passes through the attachment point of the twist body. This point is defined in both suspension systems as the middle point between the upper and the lower wishbones joint coordinates q_1 and q_2 . For each of the suspension models, a different parent-child relation between the different bodies is implemented. The parent-child structure of the Girder suspension is shown in Fig. 12.

The steer body is attached to the twist body, allowing the rotation about its z axis. The twist's body reference frame shares its y axis with the main frame's y axis. The twist body's reference frame is rotated about the y axis making coincident its x axis with the twist axis in the main frame. All the bodies after the twist body have a similar reference frame orientation. Therefore, the z axes of the twist and the steer bodies are parallel with the steering axis in the main body reference frame. The mass, the moments of inertia and the inertia products of this body correspond to those of the Girder's STR subsystem stated in the previous section. The rider's steering moment and the steering damper moment are applied to the steer body about its z axis and react on the rider's upper body and on the main body respectively. The

upper wishbone and lower wishbone bodies are children of the steer body and both rotate about the y axis. Their masses and their moments and products of inertia are obtained from the CAD designs and correspond to the Girder's UWB and LWB subsystems respectively. Finally, the suspension body is a child of the upper wishbone body and closes the four bar linkage loop with the lower wishbone at its front extreme. It also rotates about the y axis and its mass, moments and products of inertia correspond to those of the Girder's SUS subsystem. This body is the front wheel body's parent which has same properties and kinematics as the original GSX-R1000 nominal model, rotating about its y axis.

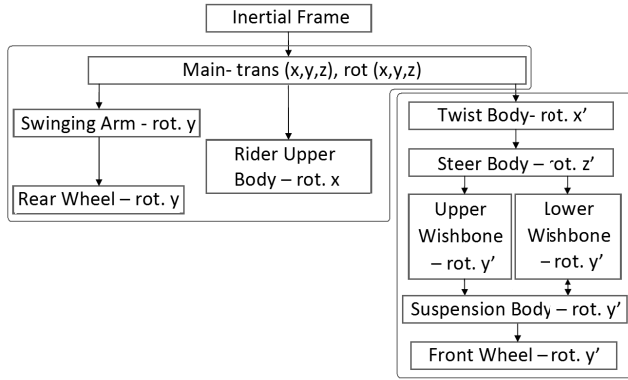


Fig. 12: Parent-child structure of the motorcycle model modified with the Girder suspension system.

Following the different mechanical configuration of the Hossack suspension system, in which the steering axle is on the four bar linkage opposite side, a different paren-child structure must now be considered. This is shown in Fig. 13. In this case, the two wishbones are connected directly to the twist body and rotate about their y axis corresponding to that of the twist body. Their mass and inertia properties were found in the previous section as those of the Hossack's UWB and LWB subsystems. The suspension body in the Hossack model also performs the system's steering action; it can rotate about its y and z axes. It is a child of the upper wishbone body and closes the four bar linkage loop with the lower linkage one. Its mass, inertia moments and inertia products (calculated through the CAD design), correspond to the Hossack SUS subsystem presented in the previous section. The front wheel body is connected to the suspension body and rotates about its y axis. It has a similar definition to that in the telescopic fork and the Girder suspension models. Considering that the inertia moment and products obtained for the Hossack STR subsystem are negligible and that it does not play a significant role on the front end kinematics, its mass is directly lumped into the main body's mass, whose centre of masses is modified according to the relative position of this subsystem. In the Hossack suspension systems, the rider's steering and the steering damper moments are directly applied to the suspension body about its z axis. The first reacts on the rider's upper body whilst the second does so on the

main body.

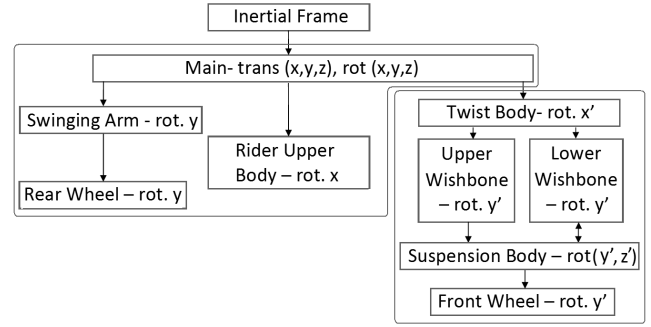


Fig. 13: Parent-child structure of the motorcycle model modified with the Hossack suspension system.

4.3 Suspension tuning

The suspension forces in both Girder and Hossack systems are modelled as two moments applied to the lower wishbones and reacting on the steer body and the twist body respectively. These suspension moments depend on the lower wishbones angular displacements and speeds, providing the reactive and the dissipative suspension actions. The focus of this work is to compare the two alternative suspension systems performance to that of the telescopic fork system. Thus, in order to introduce the minimum systems variations, it is sought a stiffness/damping tuning, for both Girder and Hossack systems, equivalent to that of the telescopic fork suspension. Following the approach in [16], the equivalent suspension moments to the linear suspension force of the telescopic fork can be calculated considering a energy conservation condition: the sum of the energy stored and dissipated by the torsional spring and damper respectively in the double wishbone system is equivalent to the linear spring and damper in the telescopic fork, for the same vertical displacement of the front wheel attachment point and in the same time. Finally, the stiffness moment and the damping coefficient are described through third order polynomial fits on the angle rotated by the lower wishbone. The damping moment results from multiply the damping coefficient and the angular rate. The maximum error achieved by this approximation is less than 2 % along the full suspension travel.

5 Suspension response

The responses of the different suspensions systems are tested and compared to the conventional telescopic fork response under two different running situation. The first considers the motorcycle passing straight through a step bump input. In the second one, the motorcycle performs a hard front braking manoeuvre. Several simulations are carried out in both cases for different motorcycle forward speeds. The results are found to be qualitatively similar for the different forward speeds under study. In here, the simulations at 40m/s are taken as example to illustrate these results.

5.1 Road bump input

The road bump input simulation is performed with the motorcycle running in straight line. After a few meters, a step input of height $h_b = 50$ mm is applied. This step bump is computed taking into account both vertical and horizontal forces appearing on the tyres when they reach the bump corner.

Figure 14 compares the front end responses to a bump input of the motorcycle fitted with a telescopic fork and with Girder and a Hossack suspension systems designed with a parallelogram (*prl*) configuration. In Fig. 14a the vertical displacement of the motorcycle handle bar is presented whilst Fig. 14b presents the vertical displacement of the front wheel centre. Although the overshoot is slightly higher for both Girder and Hossack suspension systems, it can be appreciated that the behaviours of the three models are very similar.

When both suspension systems are designed with a fork's trajectory (*tft*) configuration, the Girder system shows a response almost identical to the telescopic fork suspension case. It is the Hossack suspension system which introduces small behaviour differences. These results, shown in Fig. 15, are coherent with the fact that the steering axle in the Girder and the fork suspension systems is fixed to the chassis, and in both cases, the front wheel follows the same trajectory. Consequently, the motions of the masses in both fork and Girder systems are very close.

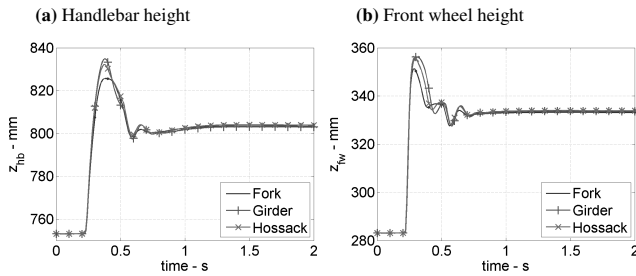


Fig. 14: Motorcycle front end response after a 50 mm road bump input with a forward speed of $v = 40$ m/s for the **parallelogram configuration (*prl*)** of both Girder and Hossack suspension systems.

Figure 16 shows the results for the road bump input simulation for the two alternative suspension systems designed in order to introduce a minimal normal trail variation (*cnt* configuration). Whilst the Hossack system response slightly differs, the Girder suspension response is closer to that of the telescopic fork.

Both alternative suspension systems have been designed to obtain similar stiffness and damping properties to the telescopic fork. However, the different mechanical configurations and mass distribution of these systems introduce small variation in the motorcycle front end response. Although a more precise tuning of each alternative suspension system would result in even more efficient response of the front end, it can be said that different kinematics configurations (*prl*, *tft*

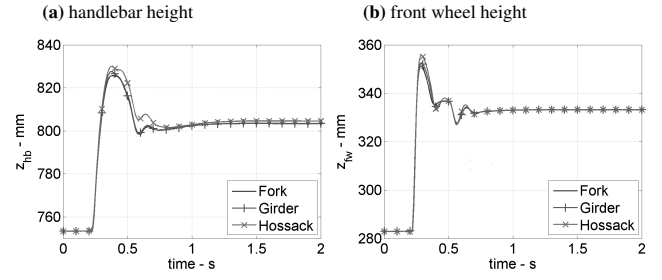


Fig. 15: Motorcycle front end response after a 50 mm road bump input with a forward speed of $v = 40$ m/s for the **telescopic fork's trajectory configuration (*tft*)** of both Girder and Hossack suspension systems.

and *cnt*) do not introduce significant variation in the suspension performance.

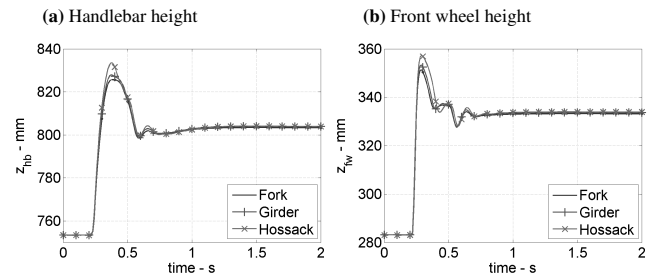


Fig. 16: Motorcycle front end response after a 50 mm road bump input with a forward speed of $v = 40$ m/s for the **constant normal trail configuration (*cnt*)** of both Girder and Hossack suspension systems.

5.2 Front wheel braking

Front wheel braking manoeuvres are simulated for a constant deceleration of $a = -0.5$ G. As it has been explained in section 2, a PD controller implemented in the model calculates the braking moment to be applied to the front wheel in order to obtain the desired deceleration. In order to focus on the pure braking effects only, the aerodynamic forces have not been taken into account by setting the drag, lift and pitch aerodynamic coefficients to zero during this simulation. The diving of the motorcycle's front end and the variation in normal trail are compared between the double wishbone suspension systems and the telescopic fork suspension.

Figure 17 shows the vertical suspension travel and the normal trail variation of the three different motorcycle models fitted with the telescopic fork, the Girder and the Hossack suspension systems with a parallelogram configuration (*prl*). The anti-dive effect is shown to increase in Fig. 17a for both double wishbone suspension systems. This is produced by their front wheels contact points trajectories which can be observed in Fig. 8. However, regarding to the normal trail variation, the Girder and Hossack systems behave opposite

to each other. Whilst the Girder suspension reaches smaller normal trail values than the telescopic fork, the Hossack system presents larger normal trail values than the fork for all the suspension travel.

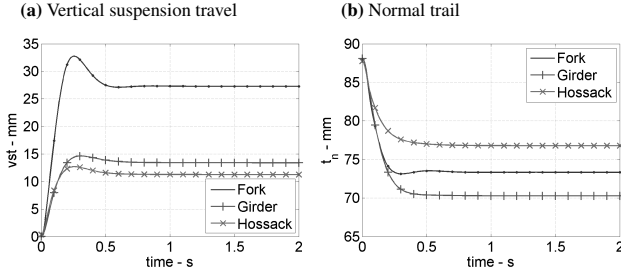


Fig. 17: Vertical suspension travel ($v.s.t.$) and normal trail (t_n) for the telescopic fork suspension compared to the Girder and Hossack systems with a **parallelogram configuration (prl)**. A straight line front wheel braking manoeuvre at an initial forward speed of $v = 40$ m/s with a constant deceleration of $a = -4.9$ m/s² is performed.

When both Girder and Hossack suspension systems are designed with a fork's trajectory configuration (tft), their diving properties become similar to those of the telescopic fork, as it is shown in Fig. 18. The vertical suspension travel reached under the braking manoeuvre is similar for the three systems. In the Girder suspension and telescopic fork cases, the common steering axles and front wheel contact points trajectories, produce similar kinematics in both systems, which results in similar normal trail behaviour.

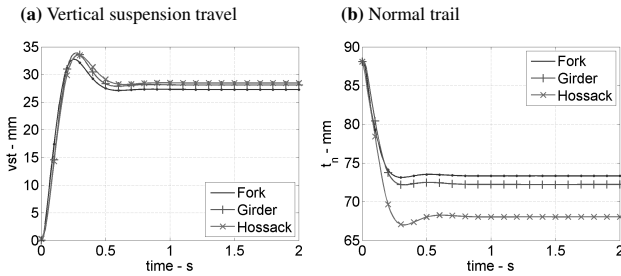


Fig. 18: Vertical suspension travel ($v.s.t.$) and normal trail (t_n) for the telescopic fork suspension compared to the Girder and Hossack systems with a **telescopic fork's trajectory configuration (tft)**. A straight line front wheel braking manoeuvre at an initial forward speed of $v = 40$ m/s with a constant deceleration of $a = -4.9$ m/s² is performed.

In the Hossack suspension system case, the normal trail is highly reduced from $t_n = 88$ mm up to $t_n = 68$ mm, which exceeds significantly the reduction of this parameter reached by the telescopic fork and Girder suspension systems. The Hossack system's geometry magnifies the normal trail reduction. In order to obtain a front wheel contact point trajectory similar to that of the telescopic fork, the steering angle is

necessarily reduced with the suspension travel. This leads to a greater normal trail reduction compared to other configurations.

Figure 19 shows the front end behaviour of the Girder and the Hossack systems configured to present a minimal normal trail variation under a front wheel braking manoeuvre. The front wheel contact point trajectory becomes highly relevant on the suspension's anti-dive effect. Looking at Fig. 10b it can be observed a trajectory of the contact point with a larger angle with the vertical that the Girder suspension produces, which makes this configuration of the Girder suspension system more prone to dive than the telescopic fork. This results in an increase of the vertical suspension travel about 10 mm with respect to the telescopic fork system.

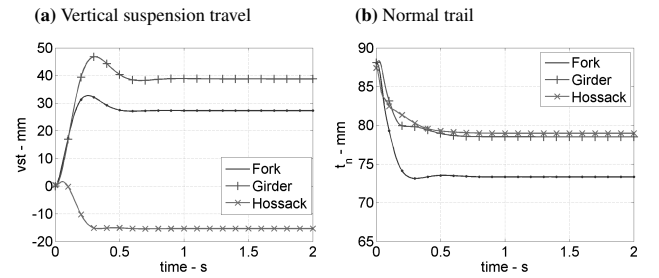


Fig. 19: Vertical suspension travel ($v.s.t.$) and normal trail (t_n) for the telescopic fork suspension compared to the Girder and Hossack systems with a **constant normal trail configuration (cnt)**. A straight line front wheel braking manoeuvre at an initial forward speed of $v = 40$ m/s with a constant deceleration of $a = -4.9$ m/s² is performed.

Conversely, the Hossack suspension system with this configuration shows a negative angle of its front wheel contact point trajectory with the vertical. This results in an opposite behaviour of the front end, which rises from its nominal position about 15 mm. Regarding to the normal trail, both Girder and Hossack suspension systems experience a reduction (limited by the geometrical configuration) of this value, as shown in Fig. 19b. Even though they were both designed to keep this value constant, this can only be achieved by considering the static suspension compression. Depending on the different accelerations on the motorcycle, other elastic parts different than those of the front suspension system will be compressed or extended: these are the tyres carcasses and the swinging arm assembly. This change in the geometry changes the kinematics design and produces a normal trail reduction, however this reduction is not as large as for the telescopic forks suspension.

Whilst the front suspension systems' kinematics do not affect in a significant manner the suspension response to a bump, it does affect the anti-dive effect and the motorcycle geometry variation under braking manoeuvres. Depending on the specifications sought, different systems may be adopted. For instance, if higher values of anti-dive and a reduction of normal trail under braking are required, then

a Girder suspension systems would provide a good kinematic solution. On the other hand, for a reduced variation of the normal trail avoiding the diving of the motorcycle while braking, a Hossack system can be used.

6 Stability analysis

In order to understand how the double wishbone suspension systems may affect the motorcycle oscillatory dynamics, stability analyses are performed taking advantage of root loci of the different linearised motorcycle models. The stability of both double wishbone suspension systems are studied for various parameter variations such as geometry configuration, front frame compliance and steering damper coefficients. Following the approach stated in section 2, the state space models derived from the linearised equations of motion are fed with the quasi-equilibrium states, integrated from the nonlinear equations. These states have been obtained for each model, from four motorcycle simulations with four different roll angles (0° , 15° , 30° and 45°). In each simulation, the forward speed is increased from 10 m/s up to 80 m/s with an acceleration of $a = 0.001 \text{ m/s}^2$.

Figure 20 shows these root loci of the nominal motorcycle model fitted with a telescopic front fork. The rider lean, weave and wobble oscillating modes are shown. Also the pitch mode appears in the area of interest, but only for the case of a 45° roll angle. The rest of the normal modes are highly damped and are not visible in this area.

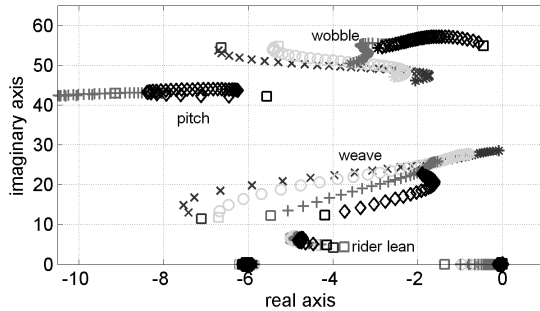


Fig. 20: Root loci of the nominal motorcycle model fitted with a telescopic fork suspension. The speed is increased from 10 m/s (\square) up to 80 m/s ($*$) at different roll angles: 0° (blue \times), 15° (green \circ), 30° (red $+$) and 45° (black \diamond).

Under straight running conditions, the rider lean, weave and wobble are out-of-plane modes whilst the pitch mode is an in-plane one. When cornering, the in-plane and out-of plane variables become coupled. The pitch mode consists in the pitching of the motorcycle through the front and rear suspension compression and extension in an almost phase opposition motion. The rider lean appears in the root locus when the rider upper-body degree of freedom is included in the mathematical model. It represents the oscillation of the rider's upper-body. The weave mode involves roll, yaw and steering angle oscillations combined in a fishtailing motion. The wobble mode is characterized by a shaking of the front

frame about the steering axis whilst the rear frame is slightly affected. The in-plane and the out-of-plane degrees of freedom become coupled for roll angles different to zero, when the motorcycle symmetry plane no longer vertical. A more extensive study of these and other modes is presented in [11]. Weave and wobble oscillating modes have been widely studied in the literature (e.g. [17], [18], [19], [20], [21], [5] just to cite a few) and they are of main relevance in this research due to their lightly-damped nature and the possibility to become unstable under some running conditions.

6.1 Geometry variation

Fitting a different suspension system may affect the motorcycle stability. However, for each suspension system under study, its geometrical configuration (*prl*, *tft* and *cnt*) does not modify in a significant manner the system's roots positions of the motorcycle fitted with that suspension. As an example Fig. 21a and Fig. 21b show the root loci for four different simulations at various motorcycle's lean angles for the Girder suspension with the telescopic fork's trajectory (*tft*) and the constant normal trail (*cnt*) configurations.

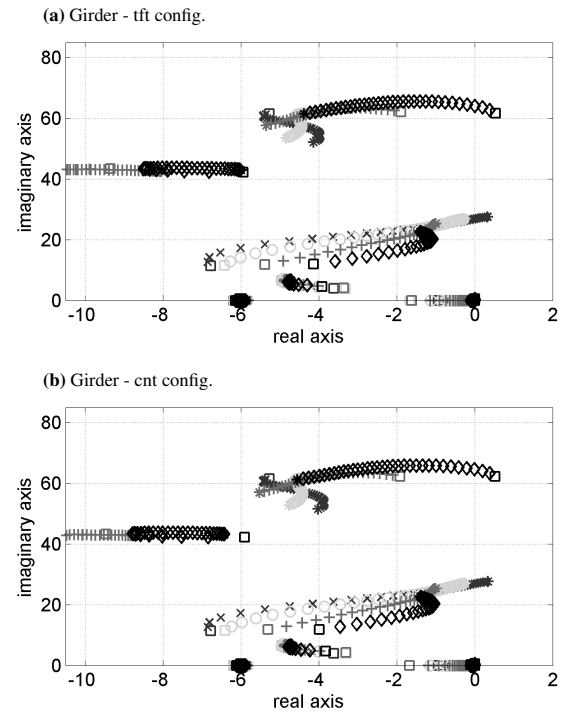


Fig. 21: Root loci of the Girder suspension for the telescopic fork's trajectory (*tft*) and the constant normal trail (*cnt*) configurations. The speed is increased from 10 m/s (\square) up to 80 m/s ($*$) at different roll angles: 0° (blue \times), 15° (green \circ), 30° (red $+$) and 45° (black \diamond).

Compared to the root loci for the telescopic fork suspension (Fig. 20), three things can be observed: first, the destabilization of the weave mode at zero roll angle for speeds above 70 m/s. At higher roll angles (15° , 30° and 45°), this mode is less damped than in the telescopic fork suspension case but

does not cross the stability limit. Secondly, the wobble mode is unstable for speeds lower than 16 m/s at 45°. However, it becomes more damped for higher speeds and smaller roll angles. Finally, the third effect of fitting the motorcycle with such a Girder suspension system is an appreciable increase of the wobble frequency. The rest of the modes remain mostly unaffected by the inclusion of this suspension system on the motorcycle model.

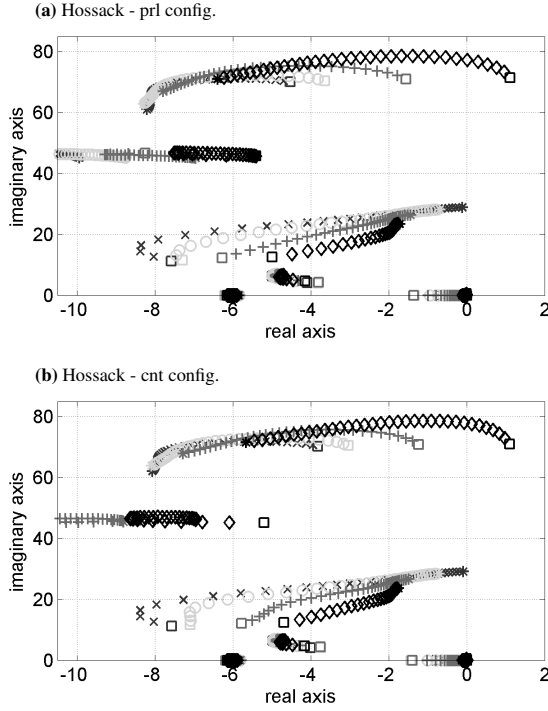


Fig. 22: Root loci of the Hossack suspension system with parallelogram (*prl*) and constant normal trail (*cnt*) configurations. The speed is increased from 10 m/s (\square) up to 80 m/s ($*$) at different roll angles: 0° (blue \times), 15° (green \circ), 30° (red $+$) and 45° (black \diamond).

On the other hand, the geometrical configuration of the Hossack system does not introduce relevant differences on the system's roots. As an example Fig. 22a and Fig. 22b show the root loci for four lean angles simulations of the Hossack suspension system with the parallelogram (*prl*) and the constant normal trail (*cnt*) configurations respectively.

Compared to the root loci of the telescopic fork suspension case, the Hossack suspension system's wobble mode becomes more damped at higher forward speeds for all roll angles whilst it is less damped at lower speeds. In the case of 45° roll angle, this mode is unstable below 20 m/s. The remaining normal modes are not substantially affected by the inclusion of this suspension system in the motorcycle model.

6.2 Front frame compliance

The design of a front suspension system will determine its compliance and hence, the stiffness at the front end. It is interesting to study how this compliance can affect the sta-

bility of a motorcycle assembly. In the GSX-R1000 nominal mathematical model, the compliance is introduced as a reacting moment applied between the chassis and the front end about the twist axis which is an axis perpendicular to the steering one and belonging to the motorcycle symmetry plane. The twist moment was defined as a torsional spring and damper combination whose stiffness and damping parameter nominal value was set to $k_{t0} = 100$ kNm and $c_{t0} = 100$ Nms. In order to study the variation on the rigidity of both front suspension systems, these stiffness and damping coefficients are modified proportionally from 60% of their nominal values up to the 140%. These maximum values may be difficult to be achieved in a real mechanical implementation, but become useful to be considered in order to highlight the trends of the system's behaviour.

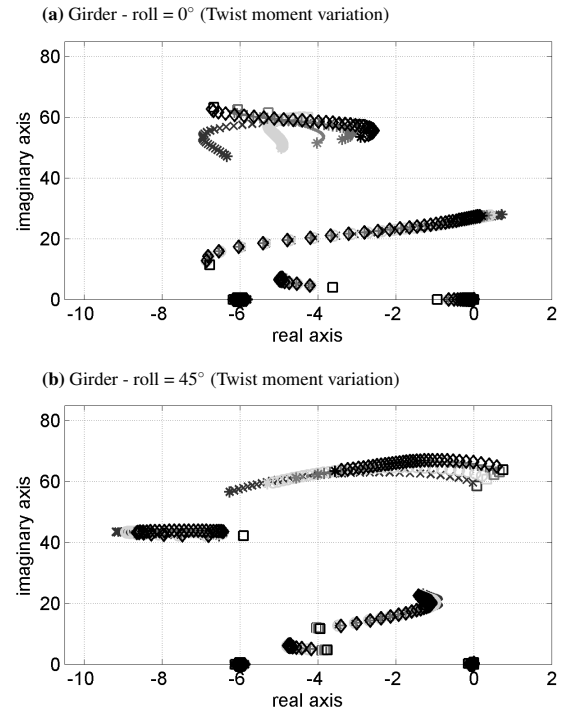


Fig. 23: Root loci for the Girder suspension system with constant normal trail (*cnt*) configuration. The twist moment coefficients are varied as 60% (blue \times), 80% (green \circ), 100% (magenta \cdot), 120% (red $+$) and 140% (black \diamond) of the nominal value. The speed is increased from 10 m/s (\square) up to 80 m/s ($*$) at different roll angles.

As it has been shown, since the variation in the geometrical configuration of both Girder and Hossack suspension systems do not affect their stability properties significantly, Figs. 23 and 24 show the root-loci of the Girder and Hossack systems for the different values of the twist moments only for the constant trail geometrical configuration. On the other hand, considering that the more relevant stability issues appear for roll angles of 0° and 45°, the root loci for 15° and 30° are not presented in order to obtain clearer results. Therefore, the root loci are plot for a unique roll angle, with different stiffness and damping coefficients values and

with the speed varied from 10 m/s up to 80 m/s.

For the Girder suspension system with nominal values of twist moment coefficients, the weave mode is unstable for speeds above 70 m/s at a zero roll angle, whilst the wobble mode instability happens for a 45° roll angle and forward speed values below 16 m/s. When the twist rigidity is increased, the wobble mode becomes more unstable whilst the weave mode's stability increases, narrowing in this way its unstable forward speed range at zero roll angle. A reduction of the twist rigidity results in the opposite effect. Consequently, weave and wobble modes stability cannot be satisfied simultaneously by modifying the front suspension system's compliance.

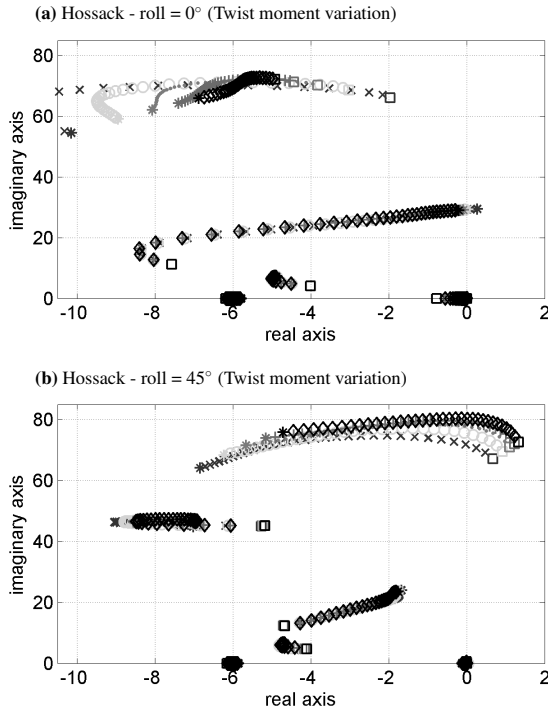


Fig. 24: Root loci for the Hossack suspension system with constant normal trail (c_{nt}) configuration. The twist moment coefficients are varied as 60%(blue \times), 80%(green \circ), 100%(magenta \cdot), 120% (red $+$) and 140% (black \diamond) of the nominal value. The speed is increased from 10 m/s (\square) up to 80 m/s ($*$) at different roll angles.

Considering the Hossack suspension system, the front end's compliance variation has an impact on the motorcycle's stability behaviour similar to that in the case of the Girder suspension. In this case, the wobble mode at 45° roll angle is stable for speed values larger than 20 m/s whilst the weave mode is stable for practically all the speed range at any roll angle for the nominal value of the twist moment coefficient. However, if the stabilization of the wobble mode for a 45° roll angle at the lower speed range is sought by decreasing the front frame's rigidity, the weave mode will become unstable for the straight line case at its higher speed range.

If these results are compared to a similar study for the telescopic fork (see Fig. 25), it can be observed that the effect

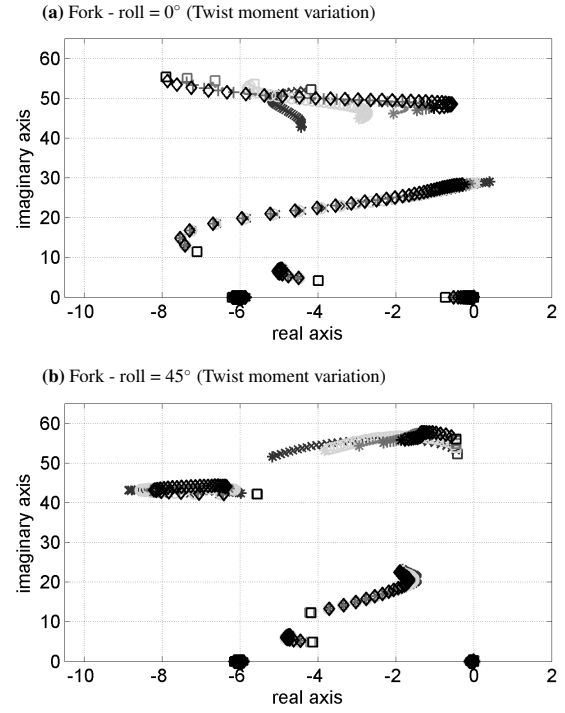


Fig. 25: Root loci for the telescopic fork suspension system. The twist moment coefficients are varied as 60%(blue \times), 80%(green \circ), 100%(magenta \cdot), 120% (red $+$) and 140% (black \diamond) of the nominal value. The speed is increased from 10 m/s (\square) up to 80 m/s ($*$) at different roll angles.

of modifying the front end's compliance on the motorcycle general stability is similar for the three suspension systems: A positive increment of the twist bending moment increases the weave mode's stability and decreases the wobble mode's stability. On the other hand, by reducing the twist bending moment the weave mode become less stable whilst the wobble mode stability is increased.

6.3 Steering damper coefficient

The steering damper is a passive device which links the steering body and the chassis; its mission is to attenuate wobble oscillations. Nowadays, a steering damper is fitted in most of the commercial sport motorcycles. The nominal GSX-R1000 model has a steering damper which is mathematically modelled as a linear reacting moment between the steering body and the motorcycle's main body (chassis).

Figures (26 - 28) show the root loci of the motorcycle system fitted with telescopic fork, Girder, Hossack suspension systems for several simulations in which the steering damper coefficient was varied from the 60 % of its nominal value ($c_{sd0} = 6.94$ Nms) up to the 140 %. For the three suspension systems the results are similar. It is well known that in the case of telescopic fork suspension systems, by increasing the steering damper coefficient the wobble mode becomes more stable, however, the weave mode stability at high forward speeds is compromised by the action of the steering damper. On the other hand, when the steering damper coefficient is reduced the effect on the motorcycle stabil-

ity is inverted ([3], [22]). Girder and Hossack systems follow the same trend in terms of stability when the damping coefficient is varied, which is to be expected.

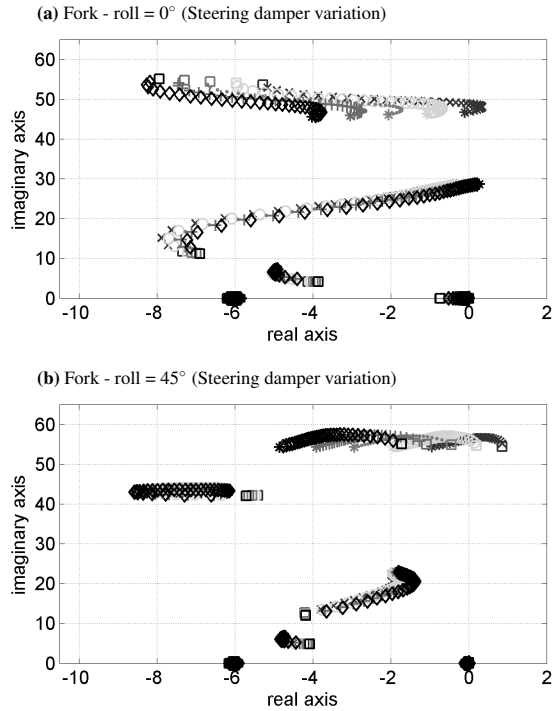


Fig. 26: Root loci for the telescopic fork suspension system. The steering damper coefficient is varied as 60%(blue \times), 80%(green \circ), 100%(magenta \cdot), 120% (red $+$) and 140% (black \diamond) of the nominal value. The speed is increased from 10 m/s (\square) up to 80 m/s ($*$) at different roll angles.

In the case of the Girder suspension, the weave mode stability is always compromised at high speeds ranges even for the smallest value of the steering damper coefficient. In this case, the wobble mode is unstable for half of the speed range at 45° roll angle. Stability of both modes cannot be achieved simultaneously with the steering damper. However, as a compromise solution, it can be used to stabilize the wobble mode at lower speed and high roll angles by sacrificing the weave stability at higher forward speed values.

It was found that for the GSX-R1000 model fitted with Girder suspension system with a constant normal trail configuration, the wobble mode becomes fully stable for a value of the steering damper coefficient of $c_{sd} = 7.85$ Ns, which is a 13 % higher than the nominal value. The maximum forward speed at which the weave mode still remains stable is $v = 70$ m/s, which for non racing conditions is a considerable speed (252 km/h) above of the allowed speed limits. On the other hand, with a Hossack suspension system, the weave mode is better damped. A steering damper coefficient value which keeps both modes stable for almost all the studied running conditions can be found for the GSX-R1000 model fitted with this suspension system. This value is $c_{sd} = 7.92$ Ns, which is a 14 % higher than the nominal value.

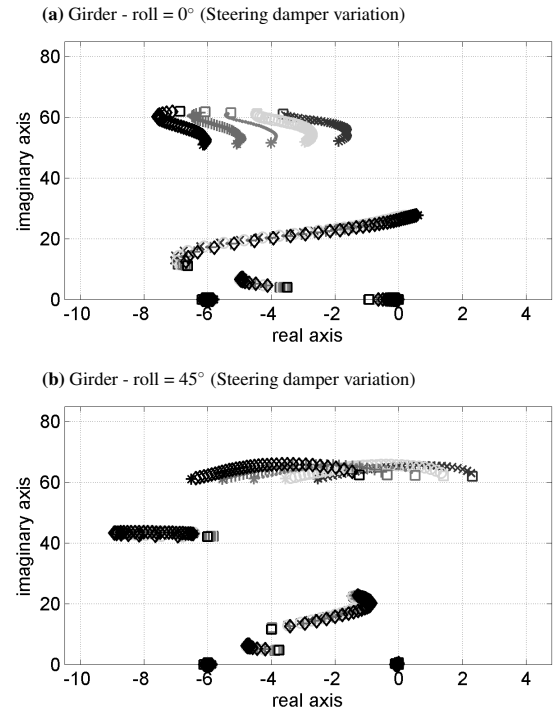


Fig. 27: Root loci for the Girder suspension system with constant normal trail (*cnt*) configuration. The steering damper coefficient is varied as 60%(blue \times), 80%(green \circ), 100%(magenta \cdot), 120% (red $+$) and 140% (black \diamond) of the nominal value. The speed is increased from 10 m/s (\square) up to 80 m/s ($*$) at different roll angles.

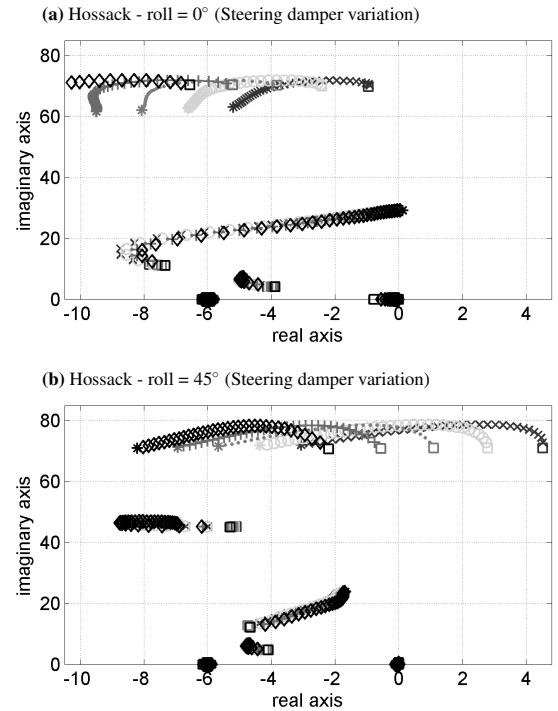


Fig. 28: Root loci for the Hossack suspension system with constant normal trail (*cnt*) configuration. The steering damper coefficient is varied as 60%(blue \times), 80%(green \circ), 100%(magenta \cdot), 120% (red $+$) and 140% (black \diamond) of the nominal value. The speed is increased from 10 m/s (\square) up to 80 m/s ($*$) at different roll angles.

6.4 Location of the front frame's centre of mass

Due to the different designs of the three suspension systems their centres of mass are differently located, as it is shown in Fig. 29.

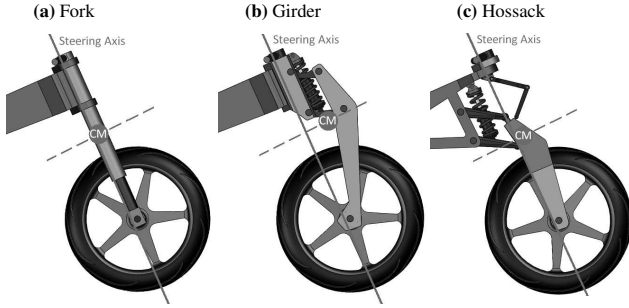


Fig. 29: Centres of mass locations of the three suspension systems.

For the telescopic fork and the Hossack suspension their centres of mass are next to the steering axis. However, in the case of the girder suspension its centre of mass is placed about 68mm ahead its steering axis.

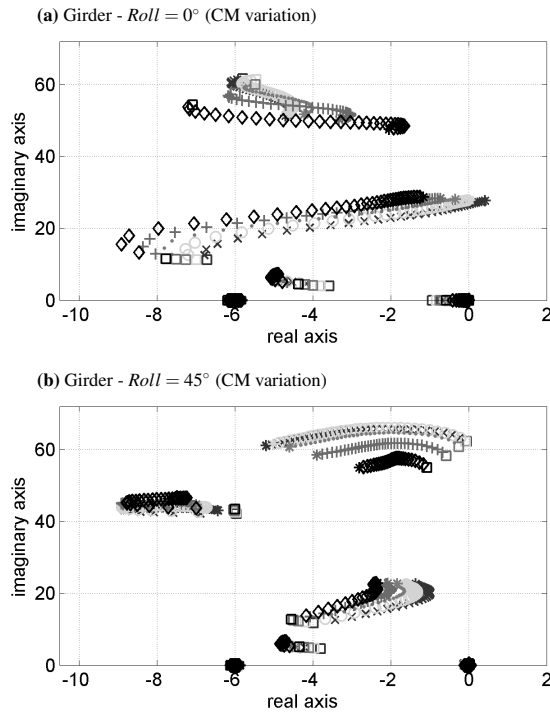


Fig. 30: Root loci for the Girder suspension system in which its centre of mass is displaced towards the steering axis. 68mm forward (blue ×), 34mm forward (green ○), 0mm (magenta ·) -34mm backwards (red +) and -68mm backwards (black ◇)

This study was made by modifying the coordinates of the centres of mass of the SUS and STR parts in the different suspension systems in order to obtain the desired assembly's

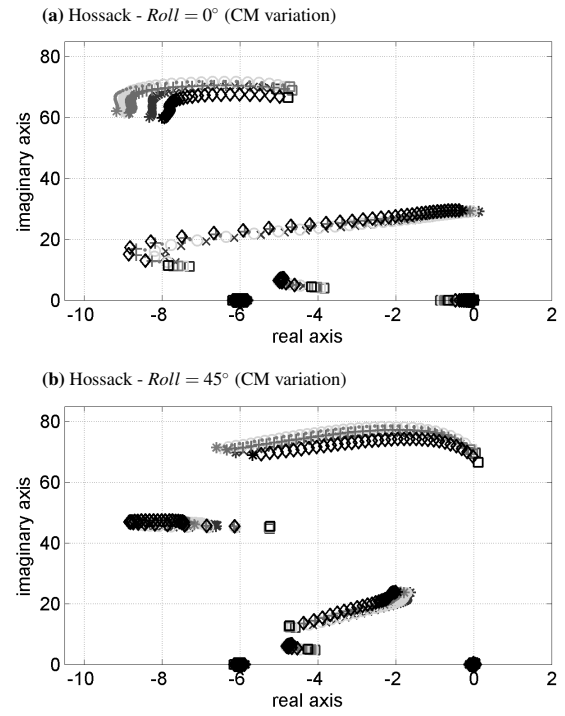


Fig. 31: Root loci for the Hossack suspension system in which its centre of mass is displaced towards the steering axis. 68mm forward (blue ×), 34mm forward (green ○), 0mm (magenta ·) -34mm backwards (red +) and -68mm backwards (black ◇)

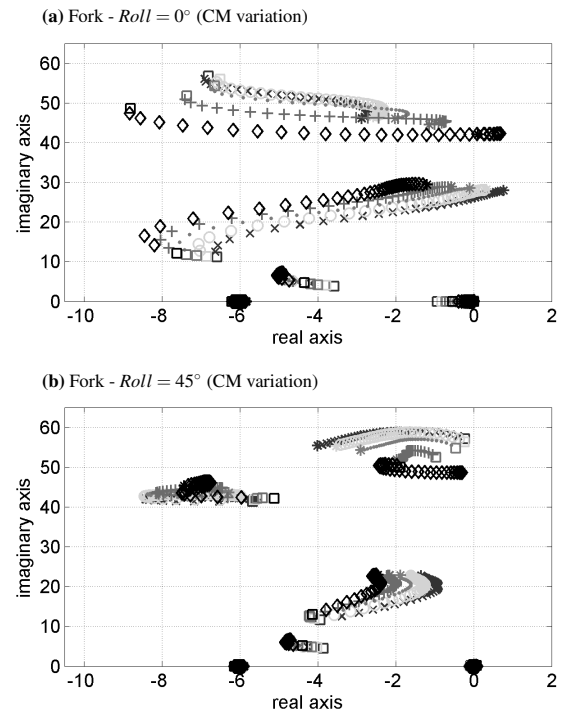


Fig. 32: Root loci for the telescopic fork suspension system in which its centre of mass is displaced towards the steering axis. 68mm forward (blue ×), 34mm forward (green ○), 0mm (magenta ·) -34mm backwards (red +) and -68mm backwards (black ◇)

centre of mass. Figure 30 presents the the impact on the root loci of displacing the centre of mass of the Girder suspension system. The distance of this point to the steering axis takes the following values: 68mm forward (blue \times), 34mm forward (green \circ), laying on the steering axis (magenta \cdot), -34mm backwards (red $+$) and -68mm backwards (black \diamond). Similar studies are performed for the Hossack and the telescopic fork suspension systems. Figure 31 and Fig 32 show these results.

For the three suspension systems it is found that, by displacing the centre of mass towards the steering axis from its nominal position, the stability of weave and wobble modes is significantly increased. The stability of the weave mode is always improved by displacing backwards the centre of mass. The wobble mode becomes more stable when the centre of mass is close to the steering axis. However, if it is displaced backwards over a certain limit the wobble mode starts to approach instability.

In both Girder and Hossack suspension system, when the centre of mass is laying on the steering axis, the weave and wobble normal modes become stable even with the nominal value of the steering damper. These results suggest that whilst a Hossack suspension system can be designed as a fully stable system just by tuning the steering damper, a Girder suspension system will present stability issues due to its geometry and mass distribution.

7 Conclusions

The main goal of this research is to understand how the different geometrical configurations of double wishbone suspension systems may affect the motorcycle dynamics. In order to do so, two different types of double wishbone suspension systems (Girder and Hossack) have been studied taking advantage of mathematical modelling and numerical simulation. The dynamic response and the stability properties of an existing motorcycle model modified with different configurations of these two suspension systems have been investigated and compared to those of the baseline model fitted with a telescopic fork suspension.

Full stability analyses were performed in order to understand how the motorcycle dynamics is affected by the front end design. The results showed that different kinematic designs of a double wishbone suspension systems do not modify the motorcycle's stability. For each of the suspension systems (Girder and Hossack), the normal modes properties remain unaffected with the three geometrical configurations. However, these normal modes differ from one suspension system to the other. It was seen that normal modes behaviour depends on dynamic parameters, such as the front frame flexibility, the steering damping coefficient and the centre of mass location, in a similar manner for the Girder, Hossack and telescopic fork suspension systems. Although each suspension system presents its particular behaviour, general properties could be obtained for the three suspension systems under study in this work.

On one hand, variations on front frame compliance affect the motorcycle's stability in an opposite manner than

the variations on the steering damper coefficient. When the steering damper coefficient is increased, the wobble mode's stability is improved whilst the weave mode stability is compromised at high speeds and small roll angles. Conversely, when the steering damper coefficient is decreased, the wobble mode stability is worsened whilst the weave mode becomes more stable. Regarding to the front frame compliance, the opposite effect is observed. Reducing system rigidity results in decreased stability of the weave mode whilst the general wobble mode stability is improved. If the systems rigidity is increased, the wobble mode become less stable and the weave mode's stability is improved.

On the other hand, the centre of mass location with respect to the steering axis of the front frame has a remarkable impact on the motorcycle stability. For the three suspension systems under study, the weave and wobble modes' stability is improved if the centre of mass is displaced backwards. The wobble mode is observed to be more stable when the centre of mass is close to the steering axis, displacing backwards the centre of mass over a certain limit reduces the stability of the wobble mode. Due to its design, the Girder suspension system has its centre of mass located in front of the steering axis farther than the other two systems. For this reason, with this suspension system, the maximum safe speed that can be reached without compromising the weave mode stability is lower than in the case of the other two systems. Although these results allow a qualitative understanding of the effect of modifying the centre of mass location in a front suspension system, the authors are currently working on designs of Girder and Hossack suspensions systems whose centres of mass lay on their steering axes, so that a full set of realistic dynamic parameters of the suspension parts can be obtained and more precise results are expected to confirm the outcomes presented in here.

Several simulations were performed to test the dynamical response of the double wishbone suspension systems. It was observed that the shock absorption capability of the three suspension systems is similar for road bump inputs. Some small differences can be observed; it has to be noted that Girder and Hossack suspensions were tuned to obtain the same equivalent stiffness and damping coefficient than those of the telescopic fork, although these coefficients are not the optimal values for the double wishbone suspension systems due to their particular designs. More precise responses would be achieved with individualized tuning of each suspension. Nevertheless, it can be said that the geometrical configuration of a double wishbone suspension system does not affect its performance in terms of shock absorption.

For front braking manoeuvres, the designs of the different suspension systems become crucial for their responses. The anti-dive capabilities of double wishbone suspension systems depend directly on the front wheel trajectory that they can perform. For the nominal parallelogram configuration (*prl*), both Girder and Hossack suspension systems have a similar responses providing some anti-dive compared to the telescopic fork. However, when both Girder and Hossack suspension systems are designed with the telescopic fork trajectory configuration (*tft*) their behaviour is similar to

that of the telescopic fork and do not provide extra anti-dive. Finally, when constant normal trail configuration (*cnt*) is implemented, the differences in the two double wishbones suspensions designs imply different behaviours. Whilst Girder suspension dives further than the telescopic fork, the Hossack system does not dives but rises. Regarding the normal trail, its variation with the suspension travel is very different for each suspension system and geometrical configuration. In the Girder suspension the steering axis is fixed to the rear frame whilst in the Hossack system this axis is fixed to the front frame. This key distinction is the cause of the differences observed in both suspension systems.

Both Girder and Hossack systems present properties in terms of anti-dive and kinematic design that can not be exploited with a telescopic fork suspension. These systems could be interesting solutions for sport motorcycles depending on the requirements of each machine. At present, the authors are conducting further research for the Girder suspension system case at high speeds.

References

- [1] Sharp, R. S., Evangelou, S., and Limebeer, D. J. N., 2004. "Advances in the modelling of motorcycle dynamics". *Multibody System Dynamics*, **12**(3), pp. pp. 251–283.
- [2] Shaeri, A., Limebeer, D. J. N., and Sharp, R. S., 2004. "Nonlinear steering oscillations of motorcycles". In *Decision and Control*, 2004. CDC. 43rd IEEE Conference on, Vol. 1, pp. 773–778 Vol.1.
- [3] Evangelou, S., Limebeer, D. J. N., Sharp, R. S., and Smith, M. C., 2006. "Mechanical steering compensators for high-performance motorcycles". *Journal of Applied Mechanics*, **74**(2), pp. pp. 332–346.
- [4] Sharp, R. S., 2007. "Motorcycle steering control by road preview". *Journal of Dynamic Systems, Measurement, and Control*, **129**(4), pp. pp. 373–382.
- [5] Evangelou, S., Limebeer, D. J., and Tomas Rodriguez, M., 2008. "Influence of road camber on motorcycle stability". *Journal of Applied Mechanics*, **75**(6), pp. pp. 061020–061020.
- [6] Evangelou, S., Limebeer, D., and Tomas-Rodriguez, M., 2010. "Suppression of burst oscillations in racing motorcycles". In *2010 49th IEEE Conference on Decision and Control (CDC)*, pp. 5578–5585.
- [7] Sharp, R. S., 2012. "Rider control of a motorcycle near to its cornering limits". *Vehicle System Dynamics*, **50**(8), pp. pp. 1–16.
- [8] Mechanical Simulation Corporation, 2015. *Vehiclesim technology*. [url: www.carsim.com](http://www.carsim.com). Accessed: 2015-05-25.
- [9] Pacejka, H. B., and Bakker, E., 1992. "The magic formula tyre model". *Vehicle System Dynamics*, **21**, pp. pp. 1–18.
- [10] Pacejka, H. B., 2002. *Tire and Vehicle Dynamics*, 2nd revised ed. Elsevier.
- [11] Moreno-Ramírez, C., 2015. "Dynamic analysis of alternative suspension systems on sport motorcycles". PhD thesis, City University London.
- [12] Sharp, R., Evangelou, S., and Limebeer, D., 2005. *Multibody aspects of motorcycle modelling with special reference to autosim*. Springer, pp. 45–68.
- [13] Evangelou, S., 2003. "The control and stability analysis of two-wheeled road vehicles". PhD thesis, University of London.
- [14] Evangelou, S. A., Limebeer, D. J. N., and Tomas-Rodriguez, M., 2012. "Suppression of burst oscillations in racing motorcycles". *Journal of Applied Mechanics*, **80**(1), pp. pp. 011003–011016.
- [15] Dassault Systems, 2015. *SolidWorks*. [url: www.solidworks.com](http://www.solidworks.com). Accessed: 2015-05-25.
- [16] Cossalter, V., 2006. *Motorcycle Dynamics*, 2nd ed. Lulu.com.
- [17] Sharp, R. S., 1971. "The stability and control of motorcycles". *Journal of Mechanical Engineering Science*, **13**(5), pp. pp. 316–329.
- [18] Cooper, K., 1974. "The effects of aerodynamics on the performance and stability of high speed motorcycles". In *2nd AIAA Symp. Aerodynamics Sport Competition Automobiles*.
- [19] Roe, G. E., and Thorpe, T. E., 1976. "A solution of the low-speed wheel flutter instability in motorcycles". *Journal of Mechanical Engineering Science*, **18**(2), pp. pp. 57–65.
- [20] Koenen, C., 1983. "The dynamic behaviour of motorcycles when running straight ahead and when cornering". PhD thesis, Delft University of Technology.
- [21] Limebeer, D. J. N., Sharp, R. S., and Evangelou, S., 2001. "The stability of motorcycles under acceleration and braking". *Journal of Mechanical Engineering Science*, **215**(9), pp. pp. 1095–1109.
- [22] Simos A. Evangelou, M. T.-R., 2014. *Motorcycle Dynamic Modes and Passive Steering Compensation in Modelling, Simulation and Control of Two-Wheeled Vehicles*, 1st ed. John Wiley and Sons, Ltd.